DOI: https://doi.org/10.15407/pmach2026.03.056

UDC 621.412

ENERGY ANALYSIS OF A SOLID OXIDE FUEL CELL – STIRLING ENGINE HYBRID POWER PLANT WITH CASCADED WASTE HEAT RECOVERY

Dmytro D. Hrinchenko
dimag628@gmail.com
ORCID: 0009-0001-8648-8099

Viktoriia O. Tarasova
vat523710@gmail.com
ORCID: 0000-0003-3252-7619

Anatolii Pidhornyi Institute of Power Machines and Systems of NAS of Ukraine,
2/10, Komunalnykiv str., Kharkiv, 61099, Ukraine

A schematic design for a hybrid power plant based on a solid oxide fuel cell (SOFC) and Stirling engines, which involves the cascaded recovery of the thermal potential of the SOFC exhaust streams, is proposed. The objective of this study is to enhance the efficiency of fuel energy utilization in the SOFC–Stirling engine hybrid power plant by developing a configuration that employs the energy potential of the SOFC exhaust streams in a cascade, recovering waste heat sequentially across Stirling engines operating at different temperature levels. A mathematical model of the system has been developed, accounting for the material and energy balances of its core components, as well as regenerator efficiency, dead volumes, and temperature differences within the Stirling engines. A parametric analysis was conducted to examine the impact of regeneration efficiency and the temperature difference between the gas stream and the working fluid on the plant's energy performance. For a configuration featuring a single Stirling engine, it was found that increasing the regenerator efficiency from 0.5 to 0.8 raises the thermal efficiency from 16.32–16.33% to 28.41–28.54%, and the electrical power output – from 116 kW to 202.72 kW. Under these conditions, the hybrid power plant achieves a maximum energy efficiency of 77.30% among the studied operating modes. It has been shown that after the first stage of waste heat recovery and the regenerative preheating of the cathode air, the temperature of the exhaust gas stream remains in the range of 474–528 °C. To utilize this thermal potential, the installation of a second Stirling engine – operating at a lower heat-input temperature level – is proposed. Calculations indicate that its electrical power output ranges from 103.29 to 108.17 kW, bringing the total electrical power output of the hybrid power plant to 810.85 kW. Among the analyzed operating modes, the highest calculated energy efficiency for the two-stage plant is 89.19%, achieved with regenerator efficiencies of $e_1=e_2=0.8$ and temperature differences of $\Delta T_{h,1}=20$ K and $\Delta T_{h,2}=50$ K. These results confirm the viability of using a cascaded approach to recover the thermal potential of SOFC exhaust streams via Stirling engines operating at different temperature levels, thereby generating additional electrical energy.

Keywords: *solid oxide fuel cell, Stirling engine, hybrid power plant, cascaded waste heat recovery, heat regeneration, temperature difference, energy efficiency.*

Introduction

Modern energy development is characterized by a transition toward decentralized energy supply systems, the integration of renewable energy sources, and increasingly stringent requirements for the energy efficiency and environmental sustainability of power generation equipment. In this context, identifying effective distributed generation technologies capable of utilizing diverse heat sources to provide stable electricity and heat production with minimal pollutant emissions has become particularly important.

The use of Stirling engines – a class of external-combustion heat engines – is considered promising in this field. A significant advantage of these engines is their ability to operate using a wide range of energy sources, including solar energy, biomass, geothermal heat, thermal storage systems, exhaust gases, and other low-grade or renewable heat sources. This makes the Stirling engine an effective component for small- and medium-scale energy systems, such as those used in microgrids, autonomous energy complexes, mobile power plants, and cogeneration systems.

Research into Stirling engines is gaining particular relevance as efforts continue to identify new design configurations for integrated energy systems that combine various heat sources, energy storage, and thermal transformation technologies. Implementing such configurations allows for improved waste heat recovery, reduced energy losses, and more efficient operation of distributed energy hubs.

This work is licensed under a Creative Commons Attribution 4.0 International License.
© Dmytro D. Hrinchenko, Viktoriia O. Tarasova, 2026

Furthermore, the use of Stirling engines in combination with thermal energy storage systems (such as solid-state or molten-salt thermal storage), solar collectors, hydrogen technologies, or cogeneration plants opens up possibilities for creating a new generation of autonomous energy systems characterized by high energy efficiency and low environmental impact.

Consequently, exploring the potential for utilizing Stirling engines within new configurations for distributed energy systems represents a relevant scientific and technical challenge, aimed at enhancing the efficiency of energy resource utilization, integrating renewable energy sources, and advancing the development of autonomous and hybrid energy systems.

Literature review on Stirling engine configurations when used in energy systems

The Stirling engine is a promising type of external-combustion heat engine that has garnered significant research interest, particularly in the context of the development of distributed energy systems, cogeneration, and the utilization of renewable energy sources. A key advantage of the Stirling engine is its ability to operate using a wide range of heat sources including solar energy, biomass, geothermal resources, industrial waste gases, and various types of fuels. This versatility makes it a promising component for small- and medium-scale energy systems designed for autonomous or decentralized power supply [1].

A substantial body of research focuses on the application of Stirling engines in small-scale cogeneration plants [1]. In such systems, the engine is used to simultaneously generate electricity and heat, which significantly increases the overall fuel utilization efficiency. An analysis of recent research indicates that micro-cogeneration plants based on Stirling engines can provide efficient energy supply for residential buildings, small enterprises, and local energy systems, thereby enhancing energy efficiency and reducing harmful emissions [2]. This paper presents an economic and environmental assessment of this technology with the aim to its implementation within Brazil's energy sector.

A distinct area of development involves the creation of combined cooling, heating and power (CCHP) systems, in which Stirling engine serves as the primary source of mechanical energy for electricity generation, while the rejected heat is utilized for providing heat supply or cooling generation via absorption or adsorption chillers. Paper [3] examines the assessment of energy efficiency and economic viability for a small-scale CCHP system designed for combined cooling, heating, and power generation with a Stirling engine. Research indicates that such systems significantly enhance the efficiency of primary energy utilization and allow for more flexible management of thermal flows within the energy supply systems of buildings and industrial facilities [3].

Another significant area is the application of Stirling engines in systems powered by renewable energy sources, most notably solar-powered Stirling engines. In these systems, thermal energy from concentrated solar radiation is directed to the engine’s heater using a parabolic dish concentrator. Studies show that such plants offer high efficiency in converting solar energy into mechanical and electrical power, making them suitable for use in remote or off-grid energy systems [4, 5].

The use of Stirling engines in biomass-based cogeneration systems also holds considerable promise. In these plants, the heat generated from the combustion of biomass or the products of its gasification is used to heat the engine's working fluid. Research indicates that combining bioenergy technologies with Stirling engines can enable the creation of efficient, low-capacity power systems for rural areas, local energy hubs, and autonomous energy supply systems [6, 7].

Another important area of application involves using the Stirling engine to recover secondary energy resources. In such configurations, the engine can utilize heat from the exhaust gases of industrial processes or internal combustion engines, thereby increasing the overall energy efficiency of technological plants and reducing heat emissions into the environment [8].

Current research also focuses on developing new integrated energy system configurations that combine the Stirling engine with Organic Rankine Cycles (ORC), heat storage systems, chillers, and other power equipment. Such combined systems enable more efficient utilization of heat flows at various temperature levels and enhance the overall efficiency of energy complexes [9].

Studies [10–11] have explored ways to improve the efficiency of Stirling engines by refining their design characteristics.

Thus, an analysis of contemporary scientific literature indicates that the Stirling engine is a promising component for distributed energy systems particularly within cogeneration, CCHP, and hybrid power plants. Future progress in this field will depend on improving the design of the engine’s heat-exchange com-

ponents, optimizing the configuration of energy systems, and integrating Stirling engines with renewable energy sources and energy storage systems.

Hybrid energy systems that combine a Stirling engine with solid oxide fuel cells (SOFC) are of particular scientific interest. The relevance of such configurations stems from the fact that SOFC operate at high temperatures, generating a significant thermal potential in the exhaust gases; this potential can be further utilized in a bottoming cycle based on a Stirling engine to produce mechanical and electrical energy. A recent review on SOFC hybridization indicates that integrating fuel cells with additional energy-conversion modules is a key strategy for enhancing the overall efficiency of stationary distributed generation systems. However, most existing research focuses on combinations involving gas turbines or internal combustion engines, while SOFC–Stirling configurations remain less explored [12].

Paper [12] provides a comprehensive overview of current trends in the hybridization of solid oxide fuel cell-based systems. Nevertheless, the emphasis is placed on combining SOFC with gas turbine plants, internal combustion engines, and other power cycles. In contrast, the integration of SOFC with a Stirling engine is addressed only tangentially, lacking a detailed analysis of system configurations, thermal interaction conditions, and the potential for effectively utilizing the heat from the fuel cell exhaust gases.

Study [13] presents a thermodynamic analysis of a hybrid SOFC–Stirling power plant utilizing alternative fuels. However, this paper focuses primarily on the overall energy efficiency of the system, whereas the optimization of the plant configuration, the parameters of heat exchange processes between the SOFC and the Stirling engine, and the impact of fuel cell exhaust gas characteristics on the engine's operating modes have been investigated to a limited extent.

In [14], a power plant configuration that combines biomass gasification, SOFC, and a Stirling engine, is proposed. The authors performed a thermodynamic and thermoeconomic analysis of the system; however, the study focuses primarily on evaluating the overall efficiency of the energy complex. The issue of optimally matching temperature levels between system components is not sufficiently addressed, nor is the potential for enhancing Stirling engine efficiency through the rational utilization of heat from the SOFC exhaust gases.

In [15], methods for improving the efficiency of a hybrid SOFC–Stirling system are investigated using finite-time thermodynamics. The analysis centers on the impact of thermodynamic losses on system efficiency. However, this paper does not explore practical design configurations for integrating a Stirling engine into distributed power generation systems, nor does it discuss the application of such plants within cogeneration or CCHP systems.

In [16], the use of a free-piston Stirling engine (FPSE) coupled with a linear electric generator is proposed as a bottoming cycle to recover high-grade heat from a solid oxide fuel cell with internal reforming. The residual heat downstream of the Stirling engine is further utilized in a double-effect absorption chiller and a heat exchanger to produce cooling and hot water. Simulation results indicate that integration of a Stirling engine increased the system's electrical efficiency by 14.1%, with the overall efficiency of the CCHP plant reaching approximately 64%. Thus, this paper confirms the viability of cascading the high-temperature heat from a solid-oxide fuel cell (SOFC) using a Stirling engine.

In paper [17], a thermodynamic analysis and multi-objective optimization were performed for a hybrid system combining SOFC, Stirling engine, and reverse osmosis plant. The heat output from the SOFC serves as a high-temperature heat source for the Stirling engine, enabling two sequential stages of electrical power generation within the system. The optimization was based on parameters such as SOFC power output, exergy efficiency, exergy destruction density, and the productivity of the desalination plant. The results demonstrate the potential of combining SOFC with Stirling engine to improve the efficiency of utilizing the high-temperature heat generated by the fuel cell.

Consequently, an analysis of papers [12–17] suggests that integrating a Stirling engine with solid-oxide fuel cells is a promising approach for enhancing the efficiency of fuel energy utilization. At the same time, further study is required for system configurations aimed at the cascaded utilization of the energy potential of SOFC exhaust streams, specifically, the recovery of residual combustible components from the anode stream, the adjustment of gas temperatures to the level required for heat input to a Stirling engine, and the subsequent utilization of the remaining thermal potential. This underscores the rationale for developing and conducting an energy analysis of a corresponding SOFC–Stirling engine hybrid power plant.

Aim and objectives of the study

The aim of the study is to improve the efficiency of fuel energy utilization in a SOFC-Stirling engine hybrid power plant by developing a system configuration that employs a cascaded approach to utilizing the energy potential of the SOFC exhaust streams, involving sequential heat recovery via Stirling engines operating at different temperature levels.

To achieve this objective, the following tasks must be addressed:

1. Development of a schematic diagram for a SOFC-Stirling engine hybrid power plant that utilizes the thermal potential of the exhaust gas streams in a cascaded manner for additional electrical power generation.

2. Proposal of a mathematical model of a hybrid plant, accounting for regeneration efficiency, the dead volumes of the Stirling engine, and the temperature differences between the heat transfer fluid and the engine's working fluid.

3. Determination of the influence of regenerator efficiency and temperature differentials in Stirling engines on their power output and the energy efficiency of the hybrid plant, and justification of the feasibility of cascaded waste heat recovery.

Development of a schematic diagram for a SOFC-Stirling engine hybrid power plant

Fuel cells are electrochemical devices that facilitate the direct conversion of the chemical energy of a fuel into electrical energy. Solid oxide fuel cells belong to the class of high-temperature fuel cells. They incorporate a solid oxide electrolyte typically made of ceramic materials such as yttria-stabilized zirconia, which enables the conduction of oxide ions within a temperature range of 600–1000 °C. Under these conditions, molecular oxygen is reduced on the porous surface of the cathode to form oxide ions, which are then transported through the electrolyte toward the anode region. Within the porous anode, these ions react with hydrogen or hydrogen-containing gases, releasing electrons that enter an external electrical circuit. Consequently, SOFC can operate using either pure hydrogen or hydrocarbon-based fuel mixtures (following a reforming process) [18].

To enhance the efficiency of fuel energy utilization, a schematic diagram for a SOFC-Stirling engine hybrid power plant has been proposed. In this configuration, the SOFC serves as the primary generator of electrical energy, while the Stirling engine functions as a bottoming recovery cycle, converting heat from the high-temperature gas stream into additional mechanical and electrical energy. This approach enables the cascaded recovery of both the fuel energy and the thermal potential inherent in the exhaust gases of the SOFC.

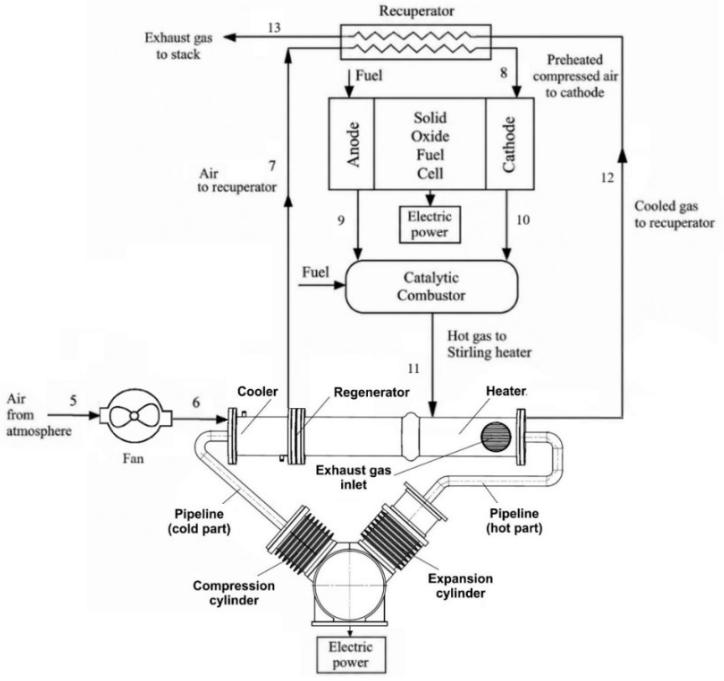


Fig. 1. Schematic diagram of a SOFC-Stirling engine hybrid power plant (a) and the Stirling engine cycle in p–v coordinates (b)

Natural gas is supplied to the fuel system of the SOFC (Fig. 1, a). Within the framework of the adopted model, fuel mixture preparation and internal steam reforming are considered as integrated processes of the SOFC system; therefore, the corresponding auxiliary components are not shown separately on the schematic diagram. The reforming process yields a hydrogen-containing fuel mixture, the components of which participate in electrochemical reactions at the SOFC anode.

Air required for the electrochemical processes at the SOFC cathode is drawn from the environment (state 5) and delivered to the plant's air system by a fan. Downstream of the fan, air (at state 6) is directed to the cold end of the Stirling engine, where it extracts heat from the engine's working fluid and is heated to state 7. Subsequently, this heated air stream (state 7) enters a recuperative heat exchanger, where it is further heated by the gas stream (state 12) exiting the Stirling engine heater; it is then delivered (at state 8) to the SOFC cathode. This configuration of the air system allows for the beneficial use of heat extracted from the cold end of the Stirling engine to preheat the cathode air.

Within the SOFC, a portion of the fuel's chemical energy is converted directly into electrical energy. Since the fuel utilization factor U_f is less than unity, the anode exhaust stream contains residual combustible components, the chemical energy of which can be utilized in a subsequent stage of energy conversion.

The anode and cathode exhaust streams, exiting the SOFC, are directed to a catalytic combustor, where residual combustible components in the anode stream are oxidized by the oxygen present in the cathode exhaust. This process generates a high-temperature gas stream at a temperature T_{11}, which is required for the efficient transfer of heat to the Stirling engine. The feasibility of using a catalytic combustor to recover energy from residual combustible components in the anode stream is supported by experimental results from the "Direct FuelCell/Turbine" hybrid plant developed by FuelCell Energy [19]. This system utilized a high-temperature carbonate fuel cell with internal natural gas reforming. Unreacted components of the anode gas were directed to a high-temperature catalytic combustor, producing a heated gas stream for subsequent use in a bottoming energy cycle. Experimental testing demonstrated that injecting additional natural gas into the low-calorific anode stream raises the gas temperature downstream of the oxidizer from 550 °C to approximately 700 °C, thereby providing the necessary thermal potential for further heat conversion.

In the proposed scheme (Fig. 1), a similar principle is applied to generate a high-temperature stream upstream of the Stirling engine heater. Unlike the plant in [19], where the heat from oxidation products is utilized in a gas-turbine cycle, in the proposed system, it is transferred to the working fluid of the Stirling engine via an external heater.

The parameters of the SOFC–Stirling engine hybrid power plant are determined for a 500 kW SOFC with internal reforming and a fuel utilization factor of U_f=0.55. The key parameters of the 500 kW SOFC model are presented in Table 1 [18].

Table 1. Key parameters of the 500 kW SOFC model

Parameter	Value
Net power plant capacity, N_{SOFC}	500 kW
Temperature at the SOFC inlet	800 °C
Temperature at the SOFC outlet	1000 °C
Pressure losses in components	1–3%
Heat losses in components	1–2%
Atmospheric pressure	1 atm.
Ambient temperature	25 °C
Fuel utilization factor, U_f	0.55

Within the framework of the adopted simplified energy model, electrochemical and chemical transformations in the SOFC are not detailed individually, as their mechanisms and the corresponding reactions are described extensively in papers [18–20]. The fraction of the fuel's chemical energy converted into electrical energy is determined by the fuel utilization factor, U_f. Consequently, not all the fuel entering the SOFC participates in the electrochemical conversion process. A portion of the combustible components remains in the anode exhaust stream, allowing for the subsequent utilization of their chemical potential within a catalytic combustor. Together with the sensible heat of the high-temperature SOFC exhaust streams, this creates a thermal potential that enables further cascaded energy utilization in a Stirling engine.

Material and heat balances of hybrid power plant components

To determine the flow parameters at key points within the schematic diagram of the SOFC–Stirling engine hybrid power plant (Fig. 1), material and heat balances for its main components have been formulated. The calculations are performed for a steady-state operating mode. Changes in the kinetic and potential energy of the flows are neglected, while heat losses from individual components are accounted for using appropriate coefficients or as terms within the heat balance equations.

A material balance equation is established for each component of the power plant

$$\sum \dot{m}_{\text{in}} = \sum \dot{m}_{\text{out}} .$$

Fan

Atmospheric air (state 5) is supplied by a fan into the plant's air system. The pressure rise across the fan is determined by the need to overcome the aerodynamic resistance of the Stirling engine's cold section, the recuperator, the SOFC cathode system, and the connecting gas ducts. In the absence of leaks, the mass flow rate of the air remains constant

$$\dot{m}_5 = \dot{m}_6 = \dot{m}_{\text{air}} .$$

The power required to drive the fan can be defined as

$$N_{\text{fan}} = \frac{\dot{m}_{\text{air}} \cdot \Delta p_{\Sigma}}{\rho_{\text{air}} \cdot \eta_{f\text{an}}},$$

where Δp_{Σ} is the total aerodynamic resistance of the air system; ρ_{air} is the air density; η_{fan} is the fan efficiency.

Recuperator

For the cold stream of the recuperator, it can be written

$$\dot{m}_7 = \dot{m}_8 = \dot{m}_{\text{air}} ,$$

and for the hot stream –

$$\dot{m}_{12} = \dot{m}_{13} .$$

Neglecting heat losses, the heat balance of the recuperator is written as

$$\dot{m}_{\text{air}} \left(h_8 - h_7\right) = \dot{m}_{12} \left(h_{12} - h_{13}\right).$$

Thus, part of the residual thermal potential of the gases after the Stirling engine returns to the cycle and is used to preheat the air entering the SOFC cathode.

Solid oxide fuel cell

Heated air with a flow rate of $\dot{m}_8$ enters the SOFC cathode, while natural gas enters the anode system with a flow rate of $\dot{m}_{\text{fuel}}$.

Within the framework of the adopted simplified flow model, the overall material balance of the SOFC is expressed as

$$\dot{m}_8 + \dot{m}_{\text{fuel}} = \dot{m}_9 + \dot{m}_{10} . \quad (1)$$

The fuel utilization factor U_f (Table 1) characterizes the fraction of the fuel stream that participates in the electrochemical conversion. Accordingly, the consumption rate of the utilized portion of the fuel is

$$\dot{m}_{\text{fuel}}^{\text{used}} = U_f \cdot \dot{m}_{\text{fuel}} .$$

Within the framework of the adopted simplified model, the flow rate of stream 9 is considered as the unconsumed fuel component leaving the anode system and is determined by the relation

$$\dot{m}_9 = (1 - U_f) \cdot \dot{m}_{\text{fuel}} . \quad (2)$$

This approach makes it possible, within a simplified model, to characterize the redistribution of the initial fuel stream between the electrochemically utilized component represented by hydrogen H_2 generated via natural gas reforming and participating in the electrochemical reaction at the SOFC anode, and the unutilized fuel component. In the actual anode exhaust stream, the latter may contain unreacted H_2, carbon monoxide CO, and residual hydrocarbon species; these retain chemical potential and can subsequently be oxidized in a catalytic combustor.

The electrical power output of the SOFC is determined by taking into account the lower heating value of the natural gas

$$N_{SOFC} = U_f \cdot \dot{m}_{\text{fuel}} \cdot Q_{LHV}^{NG} , \quad (3)$$

where $\dot{m}_{\text{fuel}}$ is the mass flow rate of natural gas; Q_{LHV}^{NG} is the lower heating value of natural gas; U_f is the fuel utilization factor.

The total energy flow entering the SOFC is determined by its electrical power

$$\dot{E}_{\text{total}} = \frac{N_{SOFC}}{\eta_{SOFC}},$$

where N_{SOFC} is the electrical power of the SOFC; η_{SOFC} is the SOFC efficiency, which is determined by the relation

$$\eta_{SOFC} = \frac{N_{SOFC}}{\dot{E}_{\text{total}}} = \frac{U_f \cdot m_{\text{fuel}} \cdot Q_{LHV}^{NG}}{\dot{m}_{\text{fuel}} \cdot Q_{LHV}^{NG}} = U_f .$$

Thus, in the simplified computational model, the energy efficiency of the SOFC is assumed to be equal to the fuel utilization factor.

A portion of the total energy flow entering the SOFC is converted into electrical energy, while the remainder determines the thermal potential of the anode and cathode exhaust streams

$$Q_{SOFC} = \dot{E}_{\text{total}} - N_{SOFC} .$$

Therefore, the heat balance can be written as

$$Q_{SOFC} = \dot{m}_9 c_{p9}(T_9 - T_8) + \dot{m}_{10} c_{p10}(T_{10} - T_8),$$

where c_{p9} and c_{p10} mean isobaric heat capacities of the anode and cathode gas streams, respectively; T_9 and T_{10} are temperatures of the anode and cathode streams at the SOFC outlet; T_8 is the air temperature at the SOFC inlet.

In the proposed scheme, the thermal and chemical potentials of the unreacted anode gases and cathode air are subsequently utilized in a catalytic combustor. The chemical energy of the residual combustible components is converted into heat, creating a high-temperature stream used to supply heat to the Stirling engine.

Catalytic combustor

The cathode and anode exhaust streams from the SOFC are directed to a catalytic combustor. The anode stream 9 contains unreacted combustible components that retain a portion of the chemical potential of the original fuel, while the cathode stream 10 contains residual oxygen not consumed in the SOFC electrochemical reactions. In the catalytic combustor, the residual combustible components of the anode stream undergo oxidation, resulting in the formation of a high-temperature gas stream 11.

The material balance for the catalytic combustor is expressed as follows

$$\dot{m}_9 + \dot{m}_{10} = \dot{m}_{11} . \tag{4}$$

Taking into account (1) and (2), equation (4) can be written as

$$\dot{m}_8 + \dot{m}_{\text{fuel}} = \dot{m}_{11} .$$

The energy balance of the catalytic combustor in the absence of additional fuel supply is written as

$$\dot{m}_{11} h_{11} = \dot{m}_9 h_9 + \dot{m}_{10} h_{10} + \dot{m}_9 Q_{LHV}^{NG},$$

at the same time

$$\dot{E}_{11} = \dot{m}_{11} h_{11}; \quad h_{11} = h(T_{11}) .$$

As a result of catalytic oxidation, a gas stream 11 is formed with a mass flow rate of $\dot{m}_{11}$ and a temperature of T_{11}, which enters the Stirling engine heater.

Stirling engine

The gas stream at state 11 enters the hot section of the Stirling engine, where it transfers heat to the engine's working fluid without direct mixing of the streams. For the gas system

$$\dot{m}_{11} = \dot{m}_{12} .$$

Thermal power transferred to the Stirling engine

$$\dot{Q}_H = \dot{m}_{11} c_p^{\text{gas}} (T_{11} - T_{12}), \tag{5}$$

where c_p^{gas} is the mean specific heat capacity of the gas stream of the catalytic combustor.

The thermal power removed from the cold section of the Stirling engine is

$$\dot{Q}_C = \dot{m}_{\text{air}} (h_7 - h_6) .$$

Analysis of the Stirling Cycle

The efficiency of a Stirling engine is determined based on a thermodynamic analysis of its operating cycle. An ideal Stirling cycle consists of two isothermal and two isochoric processes. Under the condition of ideal regeneration, the heat rejected from the working fluid during isochoric cooling is entirely stored in the regenerator and utilized during the subsequent isochoric heating. In this case, external heat input occurs only during isothermal expansion, and the theoretical efficiency of the ideal Stirling cycle is defined as

$$\eta_{id} = 1 - \frac{T_1}{T_3}, \tag{6}$$

where T_3 is the temperature of the working fluid in the hot cavity of the engine, K; T_1 is the temperature of the working fluid in the cold cavity, K.

In a real Stirling engine, efficiency is reduced due to irreversible processes, specifically, incomplete heat regeneration, imperfect heat exchange within the heater and cooler, hydraulic losses as the working fluid moves through heat-exchange components, mechanical losses, and heat losses through structure components.

This study focuses primarily on accounting for the impact of imperfect regeneration and the engine's dead volumes on the characteristics of its thermodynamic cycle.

Based on the theoretical derivations presented in [21], the useful work of a Stirling engine with imperfect regeneration and dead volumes is defined as

$$W_{\text{net}} = mR\left\{T_3 \ln\left[\frac{V_D + V_p + KT_3}{V_D + KT_3}\right] - T_1 \ln\left[\frac{V_D + V_p + KT_1}{V_D + KT_1}\right]\right\}, \tag{7}$$

where m is the total mass of the working fluid contained in the engine, kg; R is the gas constant of the working fluid, J/(kg·K); V_D and V_p are correspondingly, the displacement volume of the displacer and the working volume of the power piston, m³.

Dead volume can be expressed in terms of the total working volume

$$V_S = k_{ST} V_1 = k_{ST}(V_S + V_D + V_p),$$

where V_1 is the total volume in the state 1, m³; k_{ST} is the ratio of the total dead volume V_S to the total volume in state 1 V_1;

$$K = \left(\frac{k_{SH}}{T_3} + \frac{2k_{SR}}{T_3 + T_1} + \frac{k_{SC}}{T_1}\right) \cdot V_S,$$

where $k_{SH} = \frac{V_{SH}}{V_S}$ is the relative dead volume of the hot cavity; $k_{SR} = \frac{V_{SR}}{V_S}$ is the relative dead volume of the regenerator; $k_{SC} = \frac{V_{SC}}{V_S}$ is the relative dead volume of the cold cavity ; V_{SH}, V_{SR}, V_{SC} are dead volumes of the hot cavity, the regenerator, and the cold cavity, respectively, m³.

The coefficient K accounts for the influence of all dead volumes in the engine.

The thermal efficiency of a Stirling engine is defined as

$$\eta_t = \frac{W_{\text{net}}}{Q_{\text{in}}}.$$

Taking into account the previously derived expressions for the net work of the cycle, W_{net}, and the total heat input, Q_{in}, the thermal efficiency is determined by the expression

$$\eta_t = \frac{T_3 \ln\left[\frac{V_D + V_p + KT_3}{V_D + KT_3}\right] - T_1 \ln\left[\frac{V_D + V_p + KT_1}{V_D + KT_1}\right]}{T_3 \ln\left[\frac{V_D + V_p + KT_3}{V_D + KT_3}\right] + \frac{(T_3 - T_1)(1 - e)}{k - 1}}, \tag{8}$$

where k is the adiabatic index; e is the efficiency of an imperfect regenerator, which is determined by the formula

$$e = \frac{T_3' - T_1}{T_3 - T_1}.$$

At the same time e=1 corresponds to an efficiency of 100%, i.e. perfect regeneration, and e=0 – to a complete absence of regeneration.

The temperature of the working fluid at the regenerator outlet can be expressed in terms of its effectiveness

$$T_3' = T_1 + e(T_3 - T_1).$$

As can be seen from equation (8), the thermal efficiency of a Stirling engine depends on both the regenerator effectiveness, e, and the dead volume.

With ideal regeneration – that is, when e=1, representing the best-case scenario for Stirling cycle efficiency – and in the absence of dead volume, equation (8) is reduced to equation (6), which defines the thermal efficiency of an ideal Stirling cycle.

Thus, a Stirling engine can theoretically serve as a highly efficient device for converting heat into mechanical work, provided there is a significant temperature difference. With ideal regeneration and no dead volume, the efficiency of the Stirling cycle equals that of the Carnot cycle, which possesses the highest efficiency among all ideal thermodynamic cycles. At the same time, unlike the Carnot cycle, an engine operating on the Stirling cycle is a practically realizable heat engine that can be used to produce net work.

The work per cycle (7) is related to the engine power by the following relation

$$W_{\text{net}} = \frac{60 \cdot N_{St}}{n \cdot \eta_{\text{gen}}},$$

where n is the rotational speed, rpm; η_{gen} is the efficiency of an electric generator.

To determine the optimal operating mode for a SOFC-Stirling engine hybrid power plant, a parametric optimization problem has been formulated. The energy efficiency of the hybrid power plant is adopted as the objective function

$$\eta_{\text{hyb}} = \frac{N_{SOFC} + N_{St} - N_{\text{fan}}}{\dot{m}_{\text{fuel}} \cdot Q_{LHV}^{NG}} \to \max.$$

The varied parameters are the temperature difference on the hot side of the Stirling engine, $\Delta T_h = T_{11} - T_3$, and the efficiency of its regenerator, e.

The power output of the Stirling engine, N_{St}, is determined based on the thermodynamic analysis of its cycle, accounting for the regenerator efficiency for the various scenarios considered.

As a result, the combination of ΔT_h and e values is identified. That combination yields the maximum energy efficiency, η_{hyb}, for the hybrid power plant among the investigated operating modes.

To establish the input data for the computational model, the SOFC characteristics presented in [18] were used as a basis, specifically, a single module with a nominal electrical power output of 500 kW (Table 1).

In the first stage of the study, the electrical power consumption for the fan drive was not taken into account. This assumption allows for an assessment of the thermodynamic potential of the proposed configuration and helps determine how the temperature difference in the Stirling engine heater and the regenerator efficiency influence the energy efficiency of the hybrid power plant. Aerodynamic losses within the air system and the corresponding fan power requirements will be accounted for in a subsequent stage, during the detailed design of the heat exchangers. Table 2 presents the input data for the analysis of the SOFC-Stirling engine hybrid power plant.

Based on the assumption adopted at the first stage (that air heating within the fan is neglected) T_6=T_5=298.15 K.

For given values of T_1, T_3, the regenerator effectiveness e, and the geometric characteristics of the engine, the heat q_{in} supplied to the cycle expressed per unit mass of the working fluid is determined according to the model in [21]

$$q_{\text{in}} = \frac{Q_{\text{in}}}{m}.$$

Provided that the heat required for the implementation of the Stirling cycle is matched with the heat flux actually transferred from the combustion products and calculated by formula (5), the mass of helium is determined as

$$m = \frac{60 \cdot \dot{Q}_H}{n \cdot q_{\text{in}}}.$$

Table 2. Input data for the calculation of the SOFC-Stirling engine hybrid power plant [18, 21]

Parameter	Notation	Value
SOFC parameters		
SOFC electrical power (3)	N_{SOFC}	500 kW
Fuel utilization factor	U_f	0.55
SOFC efficiency	η_{SOFC}	0.55
Lower heating value of natural gas	Q_{LHV}^{NG}	50 MJ/kg
Air temperature at the power plant inlet	T_5	298.15 K
Air temperature at the SOFC cathode inlet	T_8	1073.15 K (800 °C)
Anode stream temperature at the SOFC outlet	T_9	1273.15 K (1000 °C)
Cathode stream temperature at the SOFC outlet	T_{10}	1273.15 K (1000 °C)
Mean isobaric heat capacity of the anode stream	c_{p9}	1.17 kJ/(kg·K)
Mean isobaric heat capacity of the cathode stream	c_{p10}	1.005 kJ/(kg·K)
Stirling engine parameters		
Working volume of the power piston	V_p	0.050 m³
Working volume of the displacer	V_D	0.075 m³
Relative dead volume of the hot space	k_{SH}	0.20
Relative dead volume of the regenerator	k_{SR}	0.60
Relative dead volume of the cold space	k_{SC}	0.20
Working fluid of the Stirling engine	—	helium
Specific gas constant of helium	R_{He}	2.0771 kJ/(kg·K)
Adiabatic index of helium	k_{He}	1.667
Specific heat capacity of helium at constant volume	C_V	3.116 kJ/(kg·K)
Engine rotational speed	n	500 rpm
Efficiency of the electric generator	η_{gen}	0.97
SOFC- Stirling engine integrating parameters		
Temperature head in the Stirling engine heater	$\Delta T_h=T_{11}-T_3$	20; 40; 60 K
Temperature head in the Stirling engine cooler	$\Delta T_c=T_1-T_6$	50 K
Temperature of the working fluid in the cold space	$T_1=T_6+\Delta T_c$	348.15 K
Temperature of the gas flow downstream of the catalytic combustor	T_{11}	calculated
Efficiency of the Stirling engine regenerator	e	0.5; 0.7; 0.8
Mean isobaric heat capacity of air	c_p^{air}	1.05 kJ/(kg·K)
Mean isobaric heat capacity of the high-temperature gas flow	c_p^{gas}	1.20 kJ/(kg·K)

Thus, the amount of helium in the working circuit is determined based on the thermal power available for recovery during a specific operating mode of the hybrid system.

Furthermore, the computational model assumes that the temperature of the high-temperature gas flow decreases by 300 K within the Stirling engine heater. Therefore, the gas temperature downstream of the heater (in K) is defined as

$$T_{12} = T_{11} - 300 .$$

This assumption makes it possible to uniquely determine the thermal power transferred to the Stirling engine and the corresponding mass of the working fluid.

Results of the calculation for a hybrid power plant without additional fuel

An algorithm developed for the calculation and parametric analysis of a SOFC-Stirling engine hybrid power plant has been implemented using the Python programming language.

The gas stream temperature downstream of the catalytic combustor was determined to be T_{11}=1405,02 K, and the thermal power delivered to the Stirling engine was found to be $\dot{Q}_{St}$=503.25 kW, given a fixed SOFC electrical power output of N_{SOFC}=500 kW. Additional results are presented in Table 3 for varying parameters of e and ΔT_h.

The analysis of the results shows that the determining parameter of the efficiency of the Stirling engine is the efficiency of the regenerator e. With its increase from 0.5 to 0.8, the thermal efficiency of the engine increases from approximately 16.32% to 28.54%, and the electrical power – from 115.94 kW to 202.72 kW. As a result, the electrical power of the hybrid power plant increases from 615.94 kW to 702.72 kW, and its energy efficiency – from 67.75% to 77.30% (Fig. 2).

Table 3. Results of the hybrid power plant calculation

ΔT_h, K	e	T_3, K	η_{St}, %	m_{He}, kg	N_{St}, kW	N_{hyb}, kW	η_{hyb}, %
20	0.5	1385.02	16.33	0.0388	116.01	616.01	67.76
20	0.7	1385.02	22.85	0.0542	162.29	662.29	72.85
20	0.8	1385.02	28.54	0.0678	202.72	702.72	77.30
40	0.5	1365.02	16.33	0.0394	115.98	615.98	67.76
40	0.7	1365.02	22.82	0.0551	162.08	662.08	72.83
40	0.8	1365.02	28.48	0.0688	202.28	702.28	77.25
60	0.5	1345.02	16.32	0.0401	115.94	615.94	67.75
60	0.7	1345.02	22.79	0.0560	161.86	661.86	72.80
60	0.8	1345.02	28.41	0.0698	201.81	701.81	77.20

Changing the temperature difference ΔT_h from 20 K to 60 K, while keeping the thermal power delivered to the Stirling engine constant, has a significantly smaller effect. As ΔT_h increases, the temperature of the working fluid T_3 decreases from 1385.02 K to 1345.02 K; however, the mass of helium required to absorb the specified thermal power increases. Consequently, the electrical power output of the engine changes only slightly. The highest value among the investigated operating modes η_{hyb}=77,3% was obtained at e=0.8 and ΔT_h=20 K.

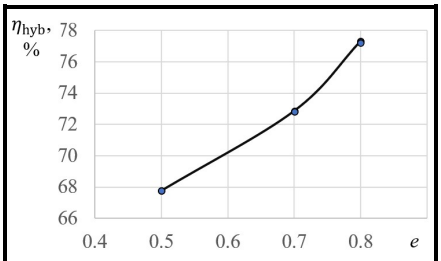


Fig. 2. Dependence of η_{hyb} on e

Table 4 presents the key temperature parameters for the flow streams in the SOFC–Stirling engine hybrid power plant, corresponding to the studied values of the temperature difference ΔT_h and the regenerator effectiveness e.

Table 4 also lists the temperatures of the gas stream downstream of the catalytic combustor T_{11}, the working fluid in the hot cavity of the Stirling engine T_3, the gas stream downstream of the heater T_{12}, the air downstream of the cold section of the engine T_7, the air at the SOFC cathode inlet T_8, and the gas stream downstream of the recuperator T_{13}.

Table 4. Key flow temperatures in the SOFC–Stirling engine hybrid power plant

ΔT_h, K	e	T_{11}, °C	T_3, °C	T_{12}, °C	T_7, °C	T_8, °C	T_{13}, °C
20	0.5	1131.87	1111.87	831.87	447.73	800	527.59
20	0.7	1131.87	1111.87	831.87	414.79	800	499.13
20	0.8	1131.87	1111.87	831.87	386.00	800	474.26
40	0.5	1131.87	1091.87	831.87	447.75	800	527.60
40	0.7	1131.87	1091.87	831.87	414.94	800	499.26
40	0.8	1131.87	1091.87	831.87	386.32	800	474.54
60	0.5	1131.87	1071.87	831.87	447.78	800	527.63
60	0.7	1131.87	1071.87	831.87	415.10	800	499.39
60	0.8	1131.87	1071.87	831.87	386.66	800	474.83

The results indicate that, following successive heat extraction in the Stirling engine heater and the recuperative heat exchanger, the temperature of flow 13 remains quite high, approximately 500 °C. This demonstrates the existence of unutilized thermal potential in the exhaust gas stream, justifying the investigation of a further stage of heat recovery, specifically, by installing a second Stirling engine designed for a lower heat-input temperature level.

Figures 3 and 4 illustrate the dependence of the new hybrid power plant's efficiency on the temperature differentials at the hot end of the first and second Stirling engines.

It can be seen from the figures that the temperature head in the second engine has a significantly greater influence on the efficiency.

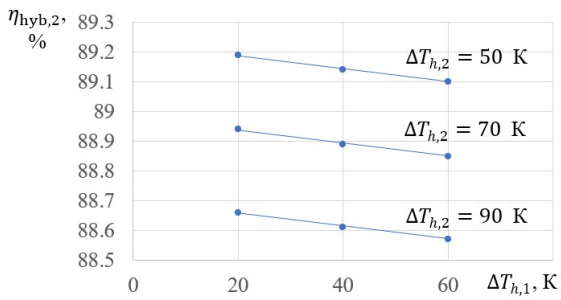


Fig. 3. Dependence of $\eta_{hyb,2}$ on $\Delta T_{h,1}$ under varied $\Delta T_{h,2}$

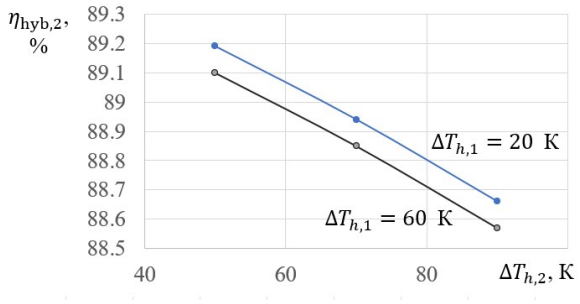


Fig. 4. Dependence of $\eta_{hyb,2}$ on $\Delta T_{h,2}$ under varied $\Delta T_{h,1}$

Discussion of Results

The calculation results indicate that the efficiency of a SOFC-Stirling engine hybrid power plant is largely determined by regeneration conditions and the temperature level at which heat is supplied to the engine. For a configuration featuring a single Stirling engine, increasing the regenerator effectiveness from e=0.5 to 0.8 results in an increase in thermal efficiency from 16.32–16.33% to 28.41–28.54%, and an increase in electrical power output from approximately 116 kW to 202 kW. Consequently, the energy efficiency of the hybrid power plant rises to 77.30%. Among the analyzed operating modes, the highest values were obtained with e=0.8 and $\Delta T_{h,1}$=20 K.

Furthermore, after the heat from the gas stream is utilized sequentially in the first Stirling engine and the recuperator, its temperature remains in the range of 474–528 °C. The existence of this temperature potential served as the basis for proposing a second stage of heat recovery, utilizing an additional Stirling engine designed for a lower temperature range.

For a two-stage configuration with e_1=e_2=0.8, it was determined that the electrical power output of the second Stirling engine ranges from 103.29 kW to 108.17 kW, depending on the assumed temperature differences. The total electrical power output of the system reaches 810.85 kW, with a calculated energy efficiency of 89.19%. Among the investigated modes, the highest values correspond to $\Delta T_{h,1}$=20 K and $\Delta T_{h,2}$=50 K. As the temperature head of the second engine increases from 50 to 90 K, its thermal efficiency and electrical power output decrease; this is attributed to a reduction in the working fluid temperature within the hot cavity.

The obtained results confirm the viability of a cascaded approach to utilizing heat from the SOFC exhaust streams. Unlike single-stage heat recovery, the proposed configuration enables the sequential utilization of the high-temperature and medium-temperature potential of the gas stream. Furthermore, the calculated efficiency values characterize the thermodynamic potential of the system under the adopted model assumptions. The current calculation does not account for fan power consumption or aerodynamic losses within the air and gas systems; these factors are intended to be incorporated during the subsequent, more detailed design phase of the system.

Conclusions

1. A schematic design for a hybrid power plant based on solid oxide fuel cells (SOFC) and Stirling engines has been developed, enabling the cascaded utilization of the thermal potential of the exhaust gas stream. It is shown that, following the first stage of waste heat recovery and the regenerative preheating of the cathode air, the gas stream temperature reaches 474–528 °C, creating the conditions for its further energy utilization.

2. It has been established that, for the first Stirling engine, the efficiency of the regenerator has the greatest impact on overall efficiency. Increasing this value from 0.5 to 0.8 raises the engine's thermal efficiency from 16.32–16.33% to 28.41–28.54%, with the maximum electrical power output among the investigated operating modes reaching 202.72 kW. The energy efficiency of the system utilizing a single Stirling engine reaches 77.30%.

3. The use of a second Stirling engine to recover the residual thermal potential of the gas stream provides an additional electrical power output of 103.29–108.17 kW. For the investigated operating modes, the total electrical power output of the system ranges from 805.15 to 810.85 kW, with a calculated energy efficiency of 88.57–89.19%.

The obtained results demonstrate the potential of cascaded waste heat recovery in SOFC–Stirling engine systems and indicate the advisability of further research, taking into account the design characteristics of the heat exchangers, aerodynamic losses, and auxiliary power consumption.

References

1. Zhu, S., Yu, G., Liang, K., Dai, W., & Luo, E. (2021). A review of Stirling-engine-based combined heat and power technology. *Applied Energy*, vol. 294, article 116965. https://doi.org/10.1016/j.apenergy.2021.116965.
2. Corria, M. E., Melian Cobas, V., & Silva Lora, E. (2006). Perspectives of Stirling engines use for distributed generation in Brazil. *Energy Policy*, vol. 34, iss. 18, pp. 3402–3408. https://doi.org/10.1016/j.enpol.2004.09.006.
3. Kong, X. Q., Wang, R. Z., & Huang, X. H. (2004). Energy efficiency and economic feasibility of CCHP driven by Stirling engine. *Energy Conversion and Management*, vol. 45, iss. 9–10, pp. 1433–1442. https://doi.org/10.1016/j.enconman.2003.09.009.
4. Kongtragool, B. & Wongwises, S. (2003). A review of solar-powered Stirling engines and low temperature differential Stirling engines. *Renewable and Sustainable Energy Reviews*, vol. 7, iss. 2, pp. 131–154. https://doi.org/10.1016/S1364-0321(02)00053-9.
5. Hossain, M. A., Parvez, M. M. H., Ahmed, I., Salekin, K. M. S., & Nahid, M. F. H. (2025). Design, fabrication, and performance evaluation of a beta-type solar-based Stirling engine for power generation. *Clean Energy*, vol. 9, iss. 4, pp. 45–53. https://doi.org/10.1093/ce/zkaf014.
6. Schneider, T., Müller, D., & Karl, J. (2020). A review of thermochemical biomass conversion combined with Stirling engines for the small-scale cogeneration of heat and power. *Renewable and Sustainable Energy Reviews*, vol. 134, article 110288. https://doi.org/10.1016/j.rser.2020.110288.
7. Cardozo, E., Erlich, C., Malmquist, A., & Alejo, L. (2014). Integration of a wood pellet burner and a Stirling engine to produce residential heat and power. *Applied Thermal Engineering*, vol. 73, iss. 1, pp. 671–680. https://doi.org/10.1016/j.applthermaleng.2014.08.024.
8. Durcansky, P., Nosek, R., & Jandacka, J. (2020). Use of Stirling engine for waste heat recovery. *Energies*, vol. 13, iss. 16, article 4133. https://doi.org/10.3390/en13164133.
9. Babamiri, A., Gharib, M., & Ebrahimi, M. (2022). Multi-criteria evaluation of a novel micro-trigeneration cycle based on α-type Stirling engine, organic Rankine cycle, and adsorption chiller. *Energy Conversion and Management*, vol. 253, article 115162. https://doi.org/10.1016/j.enconman.2021.115162.
10. Jin, X., Lü, T., Yu, G., Liu, J., & Huang, X. (2018). Design and combustion characteristic analysis of free piston Stirling engine external combustion system. *Journal of Shanghai Jiaotong University (Science)*, vol. 23, iss. 1, pp. 50–55. https://doi.org/10.1007/s12204-018-2022-x.
11. Dang, T. T., Ruellan, M., Prevond, L., Ben Ahmed, H., & Multon, B. (2015). Sizing optimization of tubular linear induction generator and its possible application in high acceleration free-piston Stirling microcogeneration. *IEEE Transactions on Industry Applications*, vol. 51, no. 5, pp. 3716–3733. https://doi.org/10.1109/TIA.2015.2427284.
12. Nikiforakis, I., Mamalis, S., & Assanis, D. (2025). Understanding solid oxide fuel cell hybridization: A critical review. *Applied Energy*, vol. 377, article 124277. https://doi.org/10.1016/j.apenergy.2024.124277.
13. Rokni, M. (2013). Thermodynamic analysis of SOFC (solid oxide fuel cell)–Stirling hybrid plants using alternative fuels. *Energy*, vol. 61, pp. 87–97. https://doi.org/10.1016/j.energy.2013.06.001.
14. Rokni, M. (2014). Thermodynamic and thermoeconomic analysis of a system with biomass gasification, solid oxide fuel cell (SOFC) and Stirling engine. *Energy*, vol. 76, pp. 19–31. https://doi.org/10.1016/j.energy.2014.01.106.
15. Lai, H.-Y., Li, Y.-T., & Chan, Y.-H. (2021). Efficiency enhancement on hybrid power system composed of irreversible solid oxide fuel cell and Stirling engine by finite time thermodynamics. *Energies*, vol. 14, iss. 4, article 1037. https://doi.org/10.3390/en14041037.
16. Majidniya, M., Remy, B., Boileau, T., & Zandi, M. (2021). Free piston Stirling engine as a new heat recovery option for an internal reforming solid oxide fuel cell. *Renewable Energy*, vol. 171, pp. 1188–1201. https://doi.org/10.1016/j.renene.2021.02.082.
17. Shakouri, O., Ahmadi, M. H., & Gord, M. F. (2021). Thermodynamic assessment and performance optimization of solid oxide fuel cell-Stirling heat engine–reverse osmosis desalination. *International Journal of Low-Carbon Technologies*, vol. 16, iss. 2, pp. 417–428. https://doi.org/10.1093/ijlct/ctaa073.
18. Welaya, Y. M. A., Mosleh, M., & Ammar, N. R. (2013). Thermodynamic analysis of a combined gas turbine power plant with a solid oxide fuel cell for marine applications. *International Journal of Naval Architecture and Ocean Engineering*, vol. 5, iss. 4, pp. 529–545. http://dx.doi.org/10.2478/IJNAOE-2013-0151.
19. Ghezel-Ayagh, H., Walzak, J., Patel, D., Daly, J., Maru, H., Sanderson, R., & Livingood, W. (2005). State of direct fuel cell/turbine systems development. *Journal of Power Sources*, vol. 152, pp. 219–225. http://dx.doi.org/10.1016/j.jpowsour.2004.12.060.
20. Larminie, J. & Dicks, A. (2003). Fuel cell systems explained. 2nd ed. Chichester: John Wiley & Sons Ltd., 406 p. https://doi.org/10.1002/9781118878330.
21. Kongtragool, B. & Wongwises, S. (2006). Thermodynamic analysis of a Stirling engine including dead volumes of hot space, cold space and regenerator. *Renewable Energy*, vol. 31, iss. 3, pp. 345–359. http://dx.doi.org/10.1016/j.renene.2005.03.012.

Received 12 August 2026 *Accepted 01 September 2026* *Published 30 September 2026*

Енергетичний аналіз гібридної установки «твердооксидний паливний елемент – двигун Стірлінга» з каскадною утилізацією теплоти

Д. Д. Грінченко, В. О. Тарасова

Інститут енергетичних машин і систем ім. А. М. Підгорного НАН України,
61099, Україна, м. Харків, вул. Комунальників, 2/10

Запропоновано схемне рішення гібридної енергетичної установки на основі твердооксидного паливного елемента (ТОПЕ) і двигунів Стірлінга, що передбачає каскадну утилізацію теплового потенціалу вихідних потоків ТОПЕ. Метою дослідження є підвищення ефективності використання енергії палива в гібридній енергетичній установці ТОПЕ – двигун Стірлінга шляхом віднайдення схемного рішення з каскадним використанням енергетичного потенціалу вихідних потоків твердооксидного паливного елемента й послідовною утилізацією теплоти в двигунах Стірлінга різного температурного рівня. Розроблено математичну модель установки, що враховує матеріальні й енергетичні баланси її основних елементів, ефективність регенератора, мертві об'єми й температурні напори в двигунах Стірлінга. Проведено параметричний аналіз впливу ефективності регенерації та температурного напору між газовим потоком і робочим тілом на енергетичні характеристики установки. Для схеми з одним двигуном Стірлінга встановлено, що збільшення ефективності регенератора від 0,5 до 0,8 підвищує його термічний ККД із 16,32–16,33% до 28,41–28,54%, а електричну потужність – з 116 до 202,72 кВт. При цьому найбільше серед досліджених режимів значення енергетичного ККД гібридної установки становить 77,30%. Показано, що після першого ступеня утилізації теплоти й рекуперативного підігрівання катодного повітря температура вихідного газового потоку залишається на рівні 474–528 °С. Для використання цього теплового потенціалу запропоновано встановлення другого двигуна Стірлінга, що працює за нижчого температурного рівня підведення теплоти. За результатами розрахунків його електрична потужність становить 103,29–108,17 кВт, а сумарна електрична потужність гібридної установки досягає 810,85 кВт. Найбільше серед досліджених режимів розрахункове значення енергетичного ККД двоступеневої установки становить 89,19% при ефективності регенераторів $e_1=e_2=0,8$ і температурних напорах $\Delta T_{h,1}=20$ K і $\Delta T_{h,2}=50$ K. Отримані результати підтверджують доцільність каскадної утилізації теплового потенціалу вихідних потоків ТОПЕ в двигунах Стірлінга різного температурного рівня для додаткового виробництва електричної енергії.

***Ключові слова**: твердооксидний паливний елемент, двигун Стірлінга, гібридна енергетична установка, каскадна утилізація теплоти, регенерація теплоти, температурний напір, енергетична ефективність.*

Література

1. Zhu S., Yu G., Liang K., Dai W., Luo E. A review of Stirling-engine-based combined heat and power technology. *Applied Energy*. 2021. Vol. 294. Article 116965. https://doi.org/10.1016/j.apenergy.2021.116965.
2. Corria M. E., Melian Cobas V., Silva Lora E. Perspectives of Stirling engines use for distributed generation in Brazil. *Energy Policy*. 2006. Vol. 34. Iss. 18. P. 3402–3408. https://doi.org/10.1016/j.enpol.2004.09.006.
3. Kong X. Q., Wang R. Z., Huang X. H. Energy efficiency and economic feasibility of CCHP driven by Stirling engine. *Energy Conversion and Management*. 2004. Vol. 45. Iss. 9–10. P. 1433–1442. https://doi.org/10.1016/j.enconman.2003.09.009.
4. Kongtragool B., Wongwises S. A review of solar-powered Stirling engines and low temperature differential Stirling engines. *Renewable and Sustainable Energy Reviews*. 2003. Vol. 7. Iss. 2. P. 131–154. https://doi.org/10.1016/S1364-0321(02)00053-9.
5. Hossain M. A., Parvez M. M. H., Ahmed I., Salekin K. M. S., Nahid M. F. H. Design, fabrication, and performance evaluation of a beta-type solar-based Stirling engine for power generation. *Clean Energy*. 2025. Vol. 9. Iss. 4. P. 45–53. https://doi.org/10.1093/ce/zkaf014.
6. Schneider T., Müller D., Karl J. A review of thermochemical biomass conversion combined with Stirling engines for the small-scale cogeneration of heat and power. *Renewable and Sustainable Energy Reviews*. 2020. Vol. 134. Article 110288. https://doi.org/10.1016/j.rser.2020.110288.
7. Cardozo E., Erlich C., Malmquist A., Alejo L. Integration of a wood pellet burner and a Stirling engine to produce residential heat and power. *Applied Thermal Engineering*. 2014. Vol. 73. Iss. 1. P. 671–680. https://doi.org/10.1016/j.applthermaleng.2014.08.024.
8. Durcansky P., Nosek R., Jandacka J. Use of Stirling engine for waste heat recovery. *Energies*. 2020. Vol. 13. Iss. 16. Article 4133. https://doi.org/10.3390/en13164133.

9. Babamiri A., Gharib M., Ebrahimi M. Multi-criteria evaluation of a novel micro-trigeneration cycle based on α-type Stirling engine, organic Rankine cycle, and adsorption chiller. *Energy Conversion and Management*. 2022. Vol. 253. Article 115162. https://doi.org/10.1016/j.enconman.2021.115162.
10. Jin X., Lü T., Yu G., Liu J., Huang X. Design and combustion characteristic analysis of free piston Stirling engine external combustion system. *Journal of Shanghai Jiaotong University (Science)*. 2018. Vol. 23. Iss. 1. P. 50–55. https://doi.org/10.1007/s12204-018-2022-x.
11. Dang T. T., Ruellan M., Prevond L., Ben Ahmed H., Multon B. Sizing optimization of tubular linear induction generator and its possible application in high acceleration free-piston Stirling microcogeneration. *IEEE Transactions on Industry Applications*. 2015. Vol. 51. No. 5. P. 3716–3733. https://doi.org/10.1109/TIA.2015.2427284.
12. Nikiforakis I., Mamalis S., Assanis D. Understanding solid oxide fuel cell hybridization: A critical review. *Applied Energy*. 2025. Vol. 377. Article 124277. https://doi.org/10.1016/j.apenergy.2024.124277.
13. Rokni M. Thermodynamic analysis of SOFC (solid oxide fuel cell)–Stirling hybrid plants using alternative fuels. *Energy*. 2013. Vol. 61. P. 87–97. https://doi.org/10.1016/j.energy.2013.06.001.
14. Rokni M. Thermodynamic and thermoeconomic analysis of a system with biomass gasification, solid oxide fuel cell (SOFC) and Stirling engine. *Energy*. 2014. Vol. 76. P. 19–31. https://doi.org/10.1016/j.energy.2014.01.106.
15. Lai H.-Y., Li Y.-T., Chan Y.-H. Efficiency enhancement on hybrid power system composed of irreversible solid oxide fuel cell and Stirling engine by finite time thermodynamics. *Energies*. 2021. Vol. 14. Iss. 4. Article 1037. https://doi.org/10.3390/en14041037.
16. Majidniya M., Remy B., Boileau T., Zandi M. Free piston Stirling engine as a new heat recovery option for an internal reforming solid oxide fuel cell. *Renewable Energy*. 2021. Vol. 171. P. 1188–1201. https://doi.org/10.1016/j.renene.2021.02.082.
17. Shakouri O., Ahmadi M. H., Gord M. F. Thermodynamic assessment and performance optimization of solid oxide fuel cell-Stirling heat engine–reverse osmosis desalination. *International Journal of Low-Carbon Technologies.* 2021. Vol. 16. Iss. 2. P. 417–428. https://doi.org/10.1093/ijlct/ctaa073.
18. Welaya Y. M. A., Mosleh M., Ammar N. R. Thermodynamic analysis of a combined gas turbine power plant with a solid oxide fuel cell for marine applications. *International Journal of Naval Architecture and Ocean Engineering*. 2013. Vol. 5. Iss. 4. P. 529–545. http://dx.doi.org/10.2478/IJNAOE-2013-0151.
19. Ghezel-Ayagh H., Walzak J., Patel D., Daly J., Maru H., Sanderson R., Livingood W. State of direct fuel cell/turbine systems development. *Journal of Power Sources*. 2005. Vol. 152. P. 219–225. http://dx.doi.org/10.1016/j.jpowsour.2004.12.060.
20. Larminie J., Dicks A. Fuel cell systems explained. 2nd ed. Chichester: John Wiley & Sons Ltd., 2003. 406 p. https://doi.org/10.1002/9781118878330.
21. Kongtragool B., Wongwises S. Thermodynamic analysis of a Stirling engine including dead volumes of hot space, cold space and regenerator. *Renewable Energy*. 2006. Vol. 31. Iss. 3. P. 345–359. http://dx.doi.org/10.1016/j.renene.2005.03.012.